



Nitrogen isotope fractionation during gas-to-particle conversion of NO_x to NO_3^- in the atmosphere – implications for isotope-based NO_x source apportionment

Yunhua Chang^{1,2,3}, Yanlin Zhang^{1,2,3}, Chongguo Tian⁴, Shichun Zhang⁵, Xiaoyan Ma⁶, Fang Cao^{1,2,3}, Xiaoyan Liu^{1,2,3}, Wenqi Zhang^{1,2,3}, Thomas Kuhn⁷, and Moritz F. Lehmann⁷

¹Yale–NUIST Center on Atmospheric Environment, International Joint Laboratory on Climate and Environment Change (ILCEC), Nanjing University of Information Science & Technology, Nanjing 210044, China

²Key Laboratory of Meteorological Disaster, Ministry of Education (KLME)/ Collaborative Innovation Center on Forecast and Evaluation of Meteorological Disasters (CIC-FEMD), Nanjing University of Information Science & Technology, Nanjing 210044, China

³Jiangsu Provincial Key Laboratory of Agricultural Meteorology, College of Applied Meteorology, Nanjing University of Information Science & Technology, Nanjing 210044, China

⁴Key Laboratory of Coastal Environmental Processes and Ecological Remediation, Yantai Institute of Coastal Zone Research, Chinese Academy of Sciences, Yantai 264003, China

⁵Northeast Institute of Geography and Agroecology, Chinese Academy of Sciences, 4888 Shengbei Road, Changchun 130102, China

⁶Key Laboratory for Aerosol-Cloud-Precipitation of China Meteorological Administration, Earth System Modeling Center, Nanjing University of Information Science and Technology, Nanjing 10044, China

⁷Aquatic and Isotope Biogeochemistry, Department of Environmental Sciences, University of Basel, 4056 Basel, Switzerland

Correspondence: Yanlin Zhang (dryanlinzhang@outlook.com, dryanlinzhang@nuist.edu.cn)

Received: 14 April 2018 – Discussion started: 8 May 2018

Revised: 31 July 2018 – Accepted: 5 August 2018 – Published: 16 August 2018

Abstract. Atmospheric fine-particle ($\text{PM}_{2.5}$) pollution is frequently associated with the formation of particulate nitrate ($p\text{NO}_3^-$), the end product of the oxidation of NO_x gases ($\text{NO} + \text{NO}_2$) in the upper troposphere. The application of stable nitrogen (N) (and oxygen) isotope analyses of $p\text{NO}_3^-$ to constrain NO_x source partitioning in the atmosphere requires knowledge of the isotope fractionation during the reactions leading to nitrate formation. Here we determined the $\delta^{15}\text{N}$ values of fresh $p\text{NO}_3^-$ ($\delta^{15}\text{N}-p\text{NO}_3^-$) in $\text{PM}_{2.5}$ at a rural site in northern China, where atmospheric $p\text{NO}_3^-$ can be attributed exclusively to biomass burning. The observed $\delta^{15}\text{N}-p\text{NO}_3^-$ ($12.17 \pm 1.55\text{‰}$; $n = 8$) was much higher than the N isotopic source signature of NO_x from biomass burning ($1.04 \pm 4.13\text{‰}$). The large difference between $\delta^{15}\text{N}-p\text{NO}_3^-$ and $\delta^{15}\text{N}-\text{NO}_x$ ($\Delta(\delta^{15}\text{N})$) can be reconciled by the net N isotope effect (ε_{N}) associated with the gas–particle conversion from NO_x to NO_3^- . For the biomass burning site, a mean ε_{N} ($\approx \Delta(\delta^{15}\text{N})$) of $10.99 \pm 0.74\text{‰}$ was assessed through a

newly developed computational quantum chemistry (CQC) module. ε_{N} depends on the relative importance of the two dominant N isotope exchange reactions involved (NO_2 reaction with OH versus hydrolysis of dinitrogen pentoxide (N_2O_5) with H_2O) and varies between regions and on a diurnal basis. A second, slightly higher CQC-based mean value for ε_{N} ($15.33 \pm 4.90\text{‰}$) was estimated for an urban site with intense traffic in eastern China and integrated in a Bayesian isotope mixing model to make isotope-based source apportionment estimates for NO_x at this site. Based on the $\delta^{15}\text{N}$ values ($10.93 \pm 3.32\text{‰}$; $n = 43$) of ambient $p\text{NO}_3^-$ determined for the urban site, and considering the location-specific estimate for ε_{N} , our results reveal that the relative contribution of coal combustion and road traffic to urban NO_x is $32\% \pm 11\%$ and $68\% \pm 11\%$, respectively. This finding agrees well with a regional bottom-up emission inventory of NO_x . Moreover, the variation pattern of OH contribution to ambient $p\text{NO}_3^-$ formation calculated by the

CQC module is consistent with that simulated by the Weather Research and Forecasting model coupled with Chemistry (WRF-Chem), further confirming the robustness of our estimates. Our investigations also show that, without the consideration of the N isotope effect during pNO₃⁻ formation, the observed δ¹⁵N–pNO₃⁻ at the study site would erroneously imply that NO_x is derived almost entirely from coal combustion. Similarly, reanalysis of reported δ¹⁵N–NO₃⁻ data throughout China and its neighboring areas suggests that NO_x emissions from coal combustion may be substantially overestimated (by > 30 %) when the N isotope fractionation during atmospheric pNO₃⁻ formation is neglected.

1 Introduction

Nitrogen oxides (NO_x = NO + NO₂) are among the most important molecules in tropospheric chemistry. They are involved in the formation of secondary aerosols and atmospheric oxidants, such as ozone (O₃) and hydroxyl radicals (OH), which control the self-cleansing capacity of the atmosphere (Galloway et al., 2003; Seinfeld and Pandis, 2012; Solomon et al., 2007). The sources of NO_x include both anthropogenic and natural origins, with more than half of the global burden (~ 40 Tg N yr⁻¹) currently attributed to fossil fuel burning (22.4–26.1 Tg N yr⁻¹) and the rest primarily derived from nitrification/denitrification in soils (including wetlands; 8.9 ± 1.9 Tg N yr⁻¹), biomass burning (5.8 ± 1.8 Tg N yr⁻¹), lightning (2–6 Tg N yr⁻¹) and oxidation of N₂O in the stratosphere (0.1–0.6 Tg N yr⁻¹) (Jaegle et al., 2005; Richter et al., 2005; Lamsal et al., 2011; Price et al., 1997; Yienger and Levy, 1995; Miyazaki et al., 2017; Duncan et al., 2016; Anenberg et al., 2017; Levy et al., 1996). The main/ultimate sinks for NO_x in the troposphere are the oxidation to nitric acid (HNO_{3(g)}) and the formation of aerosol-phase particulate nitrate (pNO₃⁻) (Seinfeld and Pandis, 2012), the partitioning of which may vary on diurnal and seasonal timescales (Morino et al., 2006).

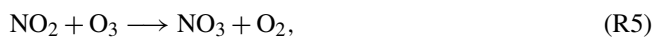
Emissions of NO_x occur mostly in the form of NO (Seinfeld and Pandis, 2012; Leighton, 1961). During daytime, transformation from NO to NO₂ is rapid (few minutes) and proceeds in a photochemical steady state, controlled by the oxidation of NO by O₃ to NO₂ and the photolysis of NO₂ back to NO (Leighton, 1961):



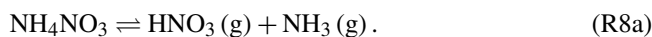
where *M* is any non-reactive species that can take up the energy released to stabilize O. NO_x oxidation to HNO₃ is governed by the following equations. During daytime,



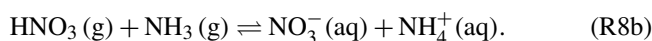
During nighttime:



HNO₃ then reacts with gas-phase NH₃ to form ammonium nitrate (NH₄NO₃) aerosols. If the ambient relative humidity (RH) is lower than the efflorescence relative humidity (ERH) or crystallization relative humidity (CRH), solid-phase NH₄NO₃(s) is formed (Smith et al., 2012; Ling and Chan, 2007):



If ambient RH exceeds the ERH or CRH, HNO₃ and NH₃ dissolve into the aqueous phase (aq) (Smith et al., 2012; Ling and Chan, 2007):



While global NO_x emissions are well constrained, individual source attribution and their local or regional role in particulate nitrate formation are difficult to assess due to the short lifetime of NO_x (typically less than 24 h) and the high degree of spatiotemporal heterogeneity with regards to the ratio between gas-phase HNO₃ and particulate NO₃⁻ (pNO₃⁻) (Duncan et al., 2016; Lu et al., 2015; Zong et al., 2017; Zhang et al., 2003). Given the conservation of the nitrogen (N) atom between NO_x sources and sinks, the N isotopic composition of pNO₃⁻ can be related to the different origins of the emitted NO_x and thus provides valuable information on the partitioning of the NO_x sources (Morin et al., 2008). Such a N isotope balance approach works best if the N isotopic composition of various NO_x sources display distinct ¹⁵N/¹⁴N ratios (reported as δ¹⁵N = $\frac{(^{15}\text{N}/^{14}\text{N})_{\text{sample}} - (^{15}\text{N}/^{14}\text{N})_{\text{N}_2}}{(^{15}\text{N}/^{14}\text{N})_{\text{N}_2}} \times 1000$).

The δ¹⁵N–NO_x of coal-fired power plant (+10‰ to +25‰) (Felix et al., 2012, 2013; Heaton, 1990), vehicle (+3.7‰ to +5.7‰) (Heaton, 1990; Walters et al., 2015; Felix and Elliott, 2014; Felix et al., 2013; Wojtal et al., 2016) and biomass burning (–7‰ to +12‰) emissions (Fibiger and Hastings, 2016), for example, is generally higher than that of lightning (–0.5‰ to +1.4‰) (Hoering, 1957) and biogenic soil (–48.9‰ to –19.9‰) emissions (Li and Wang, 2008; Felix and Elliott, 2014; Felix et al., 2013), allowing the use of isotope mixing models to gain insight on the NO_x source apportionment for gases, aerosols and the resulting nitrate deposition (–15‰ to +15‰) (Elliott et al., 2007, 2009; Zong et al., 2017; Savarino et al., 2007; Morin et al., 2008; Park et al., 2018; Altieri et al., 2013; Gobel et al., 2013). In addition, because of mass-independent fractionation during its formation (Thiemens, 1999; Thiemens and Heidenreich, 1983), ozone possesses a strong isotope anomaly (Δ¹⁷O ≈ δ¹⁷O – 0.52 × δ¹⁸O), which is propagated

into the most short-lived oxygen-bearing species, including NO_x and nitrate. Therefore, the oxygen isotopic composition of nitrate ($\delta^{18}\text{O}$, $\Delta^{17}\text{O}$) can provide information on the oxidants involved in the conversion of NO_x to nitrate (Michalski et al., 2003; Geng et al., 2017). Knopf et al. (2006, 2011) and Shiraiwa et al. (2012) have shown that NO₃ can be taken up efficiently by organic (e.g., levoglucosan) aerosol and may dominate oxidation of aerosol in the polluted urban nighttime (Kaiser et al., 2011). Globally, theoretical modeling results show that nearly 76 %, 18 % and 4 % of annual inorganic nitrate are formed via pathways/reactions involving OH, N₂O₅, and dimethyl sulfide or hydrocarbons, respectively (e.g., Alexander et al., 2009). The stable O isotopic composition of atmospheric nitrate is a powerful proxy for assessing which oxidation pathways are important for converting NO_x into nitrate under changing environmental conditions (e.g., polluted, volcanic events, climate change). Along the same lines, in this study, the average $\delta^{18}\text{O}$ value of pNO₃⁻ in Nanjing was $83.0 \pm 11.2\text{‰}$ (see Discussion section), suggesting that pNO₃⁻ formation is dominated by the pathways of “OH + NO₂” and the heterogeneous hydrolysis of N₂O₅.

$\delta^{15}\text{N}$ -based source apportionment of NO_x requires knowledge of how kinetic and equilibrium isotope fractionation may impact $\delta^{15}\text{N}$ values during the conversion of NO_x to nitrate (Freyer, 1978; Walters et al., 2016). If these isotope effects are considerable, they may greatly limit the use of $\delta^{15}\text{N}$ values of pNO₃⁻ for NO_x source partition (Walters et al., 2016). Previous studies did not take into account the potentially biasing effect of N isotope fractionation, because they assumed that changes in the $\delta^{15}\text{N}$ values during the conversion of NO_x to nitrate are minor (without detailed explanation) (Kendall et al., 2007; Morin et al., 2008; Elliott et al., 2007) or relatively small (e.g., +3 ‰) (Felix and Elliott, 2014; Freyer, 2017). However, a field study by Freyer et al. (1993) has indicated that N isotope exchange may have a strong influence on the observed $\delta^{15}\text{N}$ values in atmospheric NO and NO₂, implying that isotope equilibrium fractionation may play a significant role in shaping the $\delta^{15}\text{N}$ of NO_y species (the family of oxidized nitrogen molecules in the atmosphere, including NO_x, NO₃, NO₃⁻, peroxyacetyl nitrate, etc.). The transformation of NO_x to nitrate is a complex process that involves several different reaction pathways (Walters et al., 2016). To date, few fractionation factors for this conversion have been determined. Recently, Walters and Michalski (2015) and Walters et al. (2016) used computational quantum chemistry methods to calculate N isotope equilibrium fractionation factors for the exchange between major NO_y molecules and confirmed theoretical predictions that ¹⁵N isotopes get enriched in the more oxidized form of NO_y and that the transformation of NO_x to atmospheric nitrate (HNO₃, NO₃(aq), NO₃(g)) continuously increases the $\delta^{15}\text{N}$ in the residual NO_x pool.

As a consequence of its severe atmospheric particle pollution during the cold season, China has made great efforts to-

ward reducing NO_x emissions from on-road traffic (e.g., improving emission standards, higher gasoline quality, vehicle travel restrictions) (Li et al., 2017). Moreover, China has continuously implemented denitrogenation technologies (e.g., selective catalytic reduction) in the coal-fired power plants sector since the mid-2000s and has been phasing out small inefficient units (Liu et al., 2015). Monitoring and assessing the efficiency of such mitigation measures, and optimizing policy efforts to further reduce NO_x emissions, require knowledge of the vehicle- and power-plant-emitted NO_x to particulate nitrate in urban China (Ji et al., 2015; Fu et al., 2013; Zong et al., 2017). In this study, the chemical components of ambient fine particles (PM_{2.5}) were quantified, and the isotopic composition of particulate nitrate ($\delta^{15}\text{N}$ -NO₃⁻, $\delta^{18}\text{O}$ -NO₃⁻) was assessed in order to elucidate ambient NO_x sources in the city of Nanjing in eastern China. We also investigated the potential isotope effect during the formation of nitrate aerosols from NO_x and evaluated how disregard of such N isotope fractionation can bias N-isotope-mixing-model-based estimates on the NO_x source apportionment for nitrate deposition.

2 Methods

2.1 Field sampling

In this study, PM_{2.5} aerosol samples were collected on pre-combusted (450 °C for 6 h) quartz filters (25 × 20 cm) on a day–night basis, using high-volume air samplers at a flow rate of 1.05 m³ min⁻¹ in Sanjiang and Nanjing (Fig. 1). After sampling, the filters were wrapped in aluminum foil, packed in air-tight polyethylene bags and stored at -20 °C prior to further processing and analysis. Four blank filters were also collected. They were exposed for 10 min to ambient air (i.e., without active sampling). PM_{2.5} mass concentration was analyzed gravimetrically (Sartorius MC5 electronic microbalance) with a ±1 µg precision before and after sampling (at 25 °C and 45 % ± 5 % during weighing).

The Sanjiang campaign was performed during a period of intensive burning of agricultural residues between 8 and 18 October 2013, to examine if there is any significant difference between the $\delta^{15}\text{N}$ values of pNO₃⁻ and NO_x emitted from biomass burning. The Sanjiang site (in the following abbreviated as SJ; 47.35° N, 133.31° E) is located at an ecological experimental station affiliated with the Chinese Academy of Sciences located in the Sanjiang Plain, a major agricultural area predominantly run by state farms in northeastern China (Fig. 1). Surrounded by vast farm fields and bordering far-eastern Russia, SJ is situated in a remote and sparsely populated region, with a harsh climate and rather poorly industrialized economy. The annual mean temperature at SJ is close to the freezing point, with daily minima ranging between -31 and -15 °C in the coldest month, January. As a consequence of the relatively low tem-

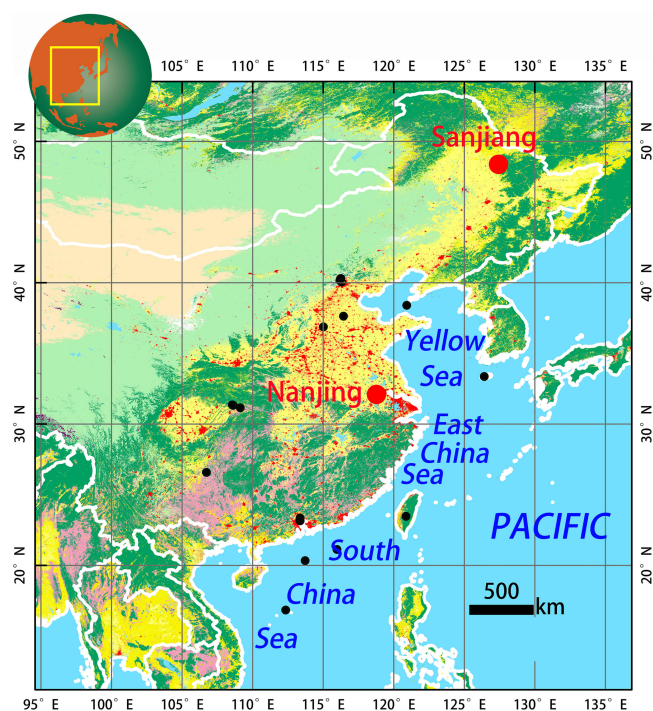


Figure 1. Location of the sampling sites Sanjiang and Nanjing. The black dots indicate the location of sampling sites (sites are located in the area of mainland China and the Yellow, East China and South China seas) with $\delta^{15}\text{N}\text{-NO}_3^-$ data from the literature (see also Table S4).

peratures (also during summer), biogenic production of NO_x through soil microbial processes is rather weak. SJ is therefore an excellent environment in which to collect biomass-burning-emitted aerosols with only minor influence from other sources.

The Nanjing campaign was conducted between 17 December 2014 and 8 January 2015 with the main objective to examine whether N isotope measurements can be used as a tool to elucidate NO_x source contributions to ambient $p\text{NO}_3^-$ during times of severe haze. Situated in the lower Yangtze River region, Nanjing is, after Shanghai, the second-largest city in eastern China. The aerosol sampler was placed at the rooftop of a building on the Nanjing University of Information Science and Technology campus (in the following abbreviated as NJ; 18 m a.g.l.; 32.21°N , 118.72°E ; Fig. 1), where NO_x emissions derive from both industrial and transportation sources.

2.1.1 Laboratory analysis

The mass concentrations of inorganic ions (including SO_4^{2-} , NO_3^- , Cl^- , NH_4^+ , K^+ , Ca^{2+} , Mg^{2+} and Na^+), carbonaceous components (organic carbon, or OC; elemental carbon, or EC) and water-soluble organic carbon were determined using an ion chromatograph (761 Compact IC, Metrohm, Switzerland), a thermal-optical OC–EC analyzer (RT-4 model, Sun-

set Laboratory Inc., USA) and a total organic carbon analyzer (Shimadzu, TOC-VCSH, Japan), respectively. Importantly, levoglucosan, a molecular marker for the biomass combustion aerosols, was detected using a Dionex™ ICS-5000+ system (Thermo Fisher Scientific, Sunnyvale, USA). Chemical aerosol analyses, including sample pre-treatment, analytical procedures, protocol adaptation, detection limits and experimental uncertainty were described in detail in our previous work (Cao et al., 2016, 2017).

For isotopic analyses of aerosol nitrate, aerosol subsamples were generated by punching 1.4 cm disks out of the filters. In order to extract the NO_3^- , sample discs were placed in acid-washed glass vials with 10 ml deionized water and placed in an ultra-sonic water bath for 30 min. Between one and four disks were used for NO_x extraction, dependent on the aerosol NO_3^- content of the filters, which was determined independently. The extracts were then filtered ($0.22\ \mu\text{m}$) and analyzed the next day. N and O isotope analyses of the extracted/dissolved aerosol nitrate ($^{15}\text{N}/^{14}\text{N}$, $^{18}\text{O}/^{16}\text{O}$) were performed using the denitrifier method (Sigman et al., 2001; Casciotti et al., 2002). Briefly, sample NO_3^- is converted to nitrous oxide (N_2O) by denitrifying bacteria that lack N_2O reductase activity (*Pseudomonas chlororaphis* ATCC 13985; formerly *Pseudomonas aureofaciens*, referred to below as such). N_2O is extracted, purified and analyzed for its N and O isotopic composition using a continuous-flow isotope ratio mass spectrometer (Thermo Finnigan Delta+, Bremen, German). Nitrate N and O isotope ratios are reported in the conventional δ notation with respect to atmospheric N_2 and Vienna standard mean ocean water, respectively. Analyses are calibrated using the international nitrate isotope standard IAEA-N3, with a $\delta^{15}\text{N}$ value of 4.7‰ and a $\delta^{18}\text{O}$ value of 25.6‰ (Böhlke et al., 2003). The blank contribution was generally lower than 0.2 nmol (as compared to 20 nmol of sample N). Based on replicate measurements of standards and samples, the analytical precision for $\delta^{15}\text{N}$ and $\delta^{18}\text{O}$ was generally better than $\pm 0.2\text{‰}$ and $\pm 0.3\text{‰}$ (1σ), respectively.

The denitrifier method generates $\delta^{15}\text{N}$ and $\delta^{18}\text{O}$ values of the combined pool of NO_3^- and NO_2^- . The presence of substantial amounts of NO_2^- in NO_3^- samples may lead to errors with regards to the analysis of $\delta^{18}\text{O}$ (Wankel et al., 2010). We refrained from including a nitrite-removal step, because nitrite concentrations in our samples were always $< 1\%$ of the NO_3^- concentrations. In the following $\delta^{15}\text{N}_{\text{NO}_x}$ and $\delta^{18}\text{O}_{\text{NO}_x}$ are thus referred to as nitrate $\delta^{15}\text{N}$ and $\delta^{18}\text{O}$ (or $\delta^{15}\text{N}_{\text{NO}_3}$ and $\delta^{18}\text{O}_{\text{NO}_3}$).

In the case of atmospheric or aerosol nitrate samples with comparatively high $\delta^{18}\text{O}$ values, $\delta^{15}\text{N}$ values tend to be overestimated by 1–2‰ (Hastings et al., 2003) if the contribution of $^{14}\text{N}^{14}\text{N}^{17}\text{O}$ to the N_2O mass 45 signal is not accounted for during isotope ratio analysis. For most natural samples, the mass-dependent relationship can be approximated as $\delta^{17}\text{O} \approx 0.52 \times \delta^{18}\text{O}$, and the $\delta^{18}\text{O}$ can be used for the ^{17}O correction. Atmospheric NO_3^- does not follow this relationship but inhabits a mass-independent component.

Thus, we adopted a correction factor of 0.8 instead of 0.52 for the ¹⁷O-to-¹⁸O linearity (Hastings et al., 2003).

2.2 Calculation of N isotope fractionation value (ε_N)

As we described above, the transformation process of NO_x to HNO₃ or NO₃⁻ involves multiple reaction pathways (see also Fig. S1 in the Supplement) and is likely to undergo isotope equilibrium exchange reactions. The measured δ¹⁵N-NO₃⁻ values of aerosol samples are thus reflective of the combined N isotope signatures of various NO_x sources (δ¹⁵N-NO_x) plus any given N isotope fractionation. Recently, Walter and Michalski (2015) used a computational quantum chemistry approach to calculate isotope exchange fractionation factors for atmospherically relevant NO_y molecules; based on this approach, Zong et al. (2017) estimated the N isotope fractionation during the transformation of NO_x to pNO₃⁻ at a regional background site in China. Here we adopted, and slightly modify, the approach by Walter and Michalski (2015) and Zong et al. (2017), and assumed that the net N isotope effect ε_N (for equilibrium processes A ↔ B: ε_{A↔B} = $\frac{(\text{heavy isotope/light isotope})_A}{(\text{heavy isotope/light isotope})_B} - 1$) · 1000‰; ε_N refers to ε_{N(NO_x↔pNO₃⁻)} in this study unless otherwise specified) during the gas-to-particle conversion from NO_x to pNO₃⁻ formation (Δ(δ¹⁵N)_{pNO₃⁻-NO_x} = δ¹⁵N-pNO₃⁻ - δ¹⁵N-NO_x ≈ ε_N) can be considered a hybrid of the isotope effects of two dominant N isotopic exchange reactions:

$$\begin{aligned} \varepsilon_N &= \gamma \times \varepsilon_{N(\text{NO}_x \leftrightarrow \text{pNO}_3^-)_{\text{OH}}} + (1 - \gamma) \times \varepsilon_{N(\text{NO}_x \leftrightarrow \text{pNO}_3^-)_{\text{H}_2\text{O}}} \\ &= \gamma \times \varepsilon_{N(\text{NO}_x \leftrightarrow \text{HNO}_3)_{\text{OH}}} + (1 - \gamma) \times \varepsilon_{N(\text{NO}_x \leftrightarrow \text{HNO}_3)_{\text{H}_2\text{O}}}, \quad (1) \end{aligned}$$

where γ represents the contribution from isotope fractionation by the reaction of NO_x and photochemically produced OH to form HNO₃ (and pNO₃⁻), as shown by ε_{N(NO_x↔HNO₃)_{OH}} (ε_{N(NO_x↔pNO₃⁻)_{OH}}). The remainder is formed by the hydrolysis of N₂O₅ with aerosol water to generate HNO₃ (and pNO₃⁻), namely, ε_{N(NO_x↔HNO₃)_{H₂O}} (ε_{N(NO_x↔pNO₃⁻)_{H₂O}}). Assuming that kinetic N isotope fractionation associated with the reaction between NO_x and OH is negligible, ε_{N(NO_x↔pNO₃⁻)_{OH}} can be calculated based on mass-balance considerations:

$$\begin{aligned} \varepsilon_{N(\text{NO}_x \leftrightarrow \text{pNO}_3^-)_{\text{OH}}} &= \varepsilon_{N(\text{NO}_x \leftrightarrow \text{HNO}_3)_{\text{OH}}} = \varepsilon_{N(\text{NO}_2 \leftrightarrow \text{HNO}_3)_{\text{OH}}} \\ &= 1000 \times \left[\frac{(^{15}\alpha_{\text{NO}_2/\text{NO}} - 1)(1 - f_{\text{NO}_2})}{(1 - f_{\text{NO}_2}) + (^{15}\alpha_{\text{NO}_2/\text{NO}} \times f_{\text{NO}_2})} \right], \quad (2) \end{aligned}$$

where ¹⁵α_{NO₂/NO} is the temperature-dependent (see Eq. 7 and Table S1 in the Supplement) equilibrium N isotope fractionation factor between NO₂ and NO, and f_{NO₂} is the fraction of NO₂ in the total NO_x. f_{NO₂} ranges from 0.2 to 0.95 (Walters and Michalski, 2015). Similarly, assuming a negligible kinetic isotope fractionation associated with the reac-

tion N₂O₅ + H₂O + aerosol → 2HNO₃, ε_{N(NO_x↔pNO₃⁻)_{H₂O}} can be computed from the following equation:

$$\begin{aligned} \varepsilon_{N(\text{NO}_x \leftrightarrow \text{pNO}_3^-)_{\text{H}_2\text{O}}} &= \varepsilon_{N(\text{NO}_x \leftrightarrow \text{HNO}_3)_{\text{H}_2\text{O}}} = \\ \varepsilon_{N(\text{NO}_x \leftrightarrow \text{N}_2\text{O}_5)_{\text{H}_2\text{O}}} &= 1000 \times (^{15}\alpha_{\text{N}_2\text{O}_5/\text{NO}_2} - 1), \quad (3) \end{aligned}$$

where ¹⁵α_{N₂O₅/NO₂} is the equilibrium isotope fractionation factor between N₂O₅ and NO₂, which also is temperature-dependent (see Eq. 7 and Table S1).

Following Walter and Michalski (2015) and Zhong et al. (2017), γ can then be approximated based on the O isotope fractionation during the conversion of NO_x to pNO₃⁻:

$$\begin{aligned} \varepsilon_{O(\text{NO}_x \leftrightarrow \text{pNO}_3^-)} &= \gamma \times \varepsilon_{O(\text{NO}_x \leftrightarrow \text{pNO}_3^-)_{\text{OH}}} \\ &+ (1 - \gamma) \times \varepsilon_{O(\text{NO}_x \leftrightarrow \text{pNO}_3^-)_{\text{H}_2\text{O}}}, \quad (4) \\ &= \gamma \times \varepsilon_{O(\text{NO}_x \leftrightarrow \text{HNO}_3)_{\text{OH}}} + (1 - \gamma) \times \varepsilon_{O(\text{NO}_x \leftrightarrow \text{HNO}_3)_{\text{H}_2\text{O}}} \end{aligned}$$

where ε_{O(NO_x↔pNO₃⁻)_{OH}} and ε_{O(NO_x↔pNO₃⁻)_{H₂O}} represent the O isotope effects associated with pNO₃⁻ generation through the reaction of NO_x and OH to form HNO₃, and the hydrolysis of N₂O₅ on a wetted surface to form HNO₃, respectively. ε_{O(NO_x↔pNO₃⁻)_{OH}} can be further expressed as

$$\begin{aligned} \varepsilon_{O(\text{NO}_x \leftrightarrow \text{pNO}_3^-)_{\text{OH}}} &= \varepsilon_{O(\text{NO}_x \leftrightarrow \text{HNO}_3)_{\text{OH}}} = \frac{2}{3} \varepsilon_{O(\text{NO}_2 \leftrightarrow \text{HNO}_3)_{\text{OH}}} \\ &+ \frac{1}{3} \varepsilon_{O(\text{NO} \leftrightarrow \text{HNO}_3)_{\text{OH}}} \\ &= \frac{2}{3} \left[\frac{1000(^{18}\alpha_{\text{NO}_2/\text{NO}} - 1)(1 - f_{\text{NO}_2})}{(1 - f_{\text{NO}_2}) + (^{18}\alpha_{\text{NO}_2/\text{NO}} \times f_{\text{NO}_2})} + (\delta^{18}\text{O} - \text{NO}_x) \right] + \\ &\frac{1}{3} \left[(\delta^{18}\text{O} - \text{H}_2\text{O}) + 1000(^{18}\alpha_{\text{OH}/\text{H}_2\text{O}} - 1) \right], \quad (5) \end{aligned}$$

and ε_{O(NO_x↔pNO₃⁻)_{H₂O}} can be determined as follows:

$$\begin{aligned} \varepsilon_{O(\text{NO}_x \leftrightarrow \text{pNO}_3^-)_{\text{H}_2\text{O}}} &= \varepsilon_{O(\text{NO}_x \leftrightarrow \text{HNO}_3)_{\text{H}_2\text{O}}} = \frac{5}{6} (\delta^{18}\text{O} - \text{N}_2\text{O}_5) \\ &+ \frac{1}{6} (\delta^{18}\text{O} - \text{H}_2\text{O}), \quad (6) \end{aligned}$$

where ¹⁸α_{NO₂/NO} and ¹⁸α_{OH/H₂O} represent the equilibrium O isotope fractionation factors between NO₂ and NO between and OH and H₂O, respectively. The range of δ¹⁸O-H₂O can be approximated using an estimated tropospheric water vapor δ¹⁸O range of -25‰ to 0‰. The δ¹⁸O values for NO₂ and N₂O₅ range from 90‰ to 122‰ (Zong et al., 2017).

¹⁵α_{NO₂/NO}, ¹⁵α_{N₂O₅/NO₂}, ¹⁸α_{NO₂/NO} and ¹⁸α_{OH/H₂O} in these equations are dependent on the temperature, which can be expressed as

$$1000(m\alpha_{X/Y} - 1) = \frac{A}{T^4} \times 10^{10} + \frac{B}{T^3} \times 10^8 + \frac{C}{T^2} \times 10^6 + \frac{D}{T} \times 10^4, \quad (7)$$

where *A*, *B*, *C* and *D* are experimental constants (Table S1 in the Supplement) over the temperature range of 150–450 K (Walters and Michalski, 2015; Walters et al., 2016; Walters and Michalski, 2016; Zong et al., 2017).

Based on Eqs. (4)–(7) and measured values for δ¹⁸O–pNO₃⁻ of ambient PM_{2.5}, a Monte Carlo simulation was performed to generate 10 000 feasible solutions. The error between predicted and measured δ¹⁸O was less than 0.5‰. The range (maximum and minimum) of computed contribution ratios (*γ*) was then integrated in Eq. (1) to generate an estimate range for the nitrogen isotope effect ε_N (using Eqs. 2–3). δ¹⁵N–pNO₃⁻ values can be calculated based on ε_N and the estimated δ¹⁵N range for atmospheric NO_x (see Sect. 2.4).

2.3 Bayesian isotope mixing model

Isotopic mixing models allow estimating the relative contribution of multiple sources (e.g., emission sources of NO_x) within a mixed pool (e.g., ambient pNO₃⁻). By explicitly considering the uncertainty associated with the isotopic signatures of any given source, as well as isotope fractionation during the formation of various components of a mixture, the application of Bayesian methods to stable isotope mixing models generates robust probability estimates of source proportions and is often more appropriate when targeting natural systems than simple linear mixing models (Chang et al., 2016a). Here the Bayesian model MixSIR (a stable isotope mixing model using sampling, importance and resampling) was used to disentangle multiple NO_x sources by generating potential solutions of source apportionment as true probability distributions, which has been widely applied in a number of fields (e.g., Parnell et al., 2013; Phillips et al., 2014; Zong et al., 2017). Details on the model frame and computing methods are given in Sect. S1 in the Supplement.

Here, coal combustion (13.72 ± 4.57‰), transportation (−3.71 ± 10.40‰), biomass burning (1.04 ± 4.13‰) and biogenic emissions from soils (−33.77 ± 12.16‰) were considered to be the most relevant contributors of NO_x (Table S2 and Sect. S2). The δ¹⁵N of atmospheric NO_x is unknown. However, it can be assumed that its range in the atmosphere is constrained by the δ¹⁵N of the NO_x sources and the δ¹⁵N of pNO₃⁻ after equilibrium fractionation conditions have been reached. Following Zong et al. (2017), δ¹⁵N–NO_x in the atmosphere was determined by performing iterative model simulations, with a simulation step of 0.01 times the equilibrium fractionation value based on the δ¹⁵N–NO_x values of the emission sources (mean and standard deviation) and the measured δ¹⁵N–pNO₃⁻ of ambient PM_{2.5} (Fig. S2).

3 Results

3.1 Sanjiang in northern China

The δ¹⁵N–pNO₃⁻ and δ¹⁸O–pNO₃⁻ values of the eight samples collected from the Sanjiang biomass burning field experiment ranged from 9.54‰ to 13.77‰ (mean: 12.17‰) and 57.17‰ to 75.09‰ (mean: 63.57‰), respectively. In this study, atmospheric concentrations of levoglucosan quantified from PM_{2.5} samples collected near the sites of biomass burning in Sanjiang vary between 4.0 and 20.5 μg m⁻³, 2 to 5 orders of magnitude higher than those measured during non-biomass-burning season (Cao et al., 2017, 2016). Levoglucosan is an anhydrosugar formed during pyrolysis of cellulose at temperatures above 300 °C (Simoneit, 2002). Due to its specificity for cellulose combustion, it has been widely used as a molecular tracer for biomass burning (Simoneit et al., 1999; D. Liu et al., 2013; Jedynska et al., 2014; Liu et al., 2014). Indeed, the concentrations of levoglucosan and aerosol nitrate in Sanjiang were highly correlated (*R*² = 0.64; Fig. 2a), providing compelling evidence that particulate nitrate measured during our study period was predominately derived from biomass burning emissions.

3.2 Nanjing in eastern China

The mass concentrations (mean_{min}^{max} ± 1σ, *n* = 43) of PM_{2.5} and pNO₃⁻ measured in Nanjing were 122.1_{39.0}^{227.8} ± 47.9 and 17.8_{4.0}^{45.2} ± 10.3 μg m⁻³, respectively. All PM_{2.5} concentrations exceeded the Chinese Air Quality Standards for daily PM_{2.5} (35 μg m⁻³), suggesting severe haze pollution during the sampling period. The corresponding δ¹⁵N–pNO₃⁻ values (raw data without correction) ranged between 5.39‰ and 17.99‰, indicating significant enrichment in ¹⁵N relative to rural and coastal marine atmospheric NO₃⁻ sources (Table S4). This may be due to the prominent contribution of fossil-fuel-related NO_x emissions with higher δ¹⁵N values in urban areas (Elliott et al., 2007; Park et al., 2018).

4 Discussion

4.1 Sanjiang campaign: theoretical calculation and field validation of N isotope fractionation during pNO₃⁻ formation

To be used as a quantitative tracer of biomass-combustion-generated aerosols, levoglucosan must be conserved during its transport from its source, without partial removal by reactions in the atmosphere (Hennigan et al., 2010). The mass concentrations of non-sea-salt potassium (nss-K⁺ = K⁺ − 0.0355 × Na⁺) is considered as an independent/additional indicator of biomass burning (Fig. 2b). The association of elevated levels of levoglucosan with high nss-K⁺ concentrations underscores that the two compounds derived from the same proximate sources and thus that aerosol levoglu-

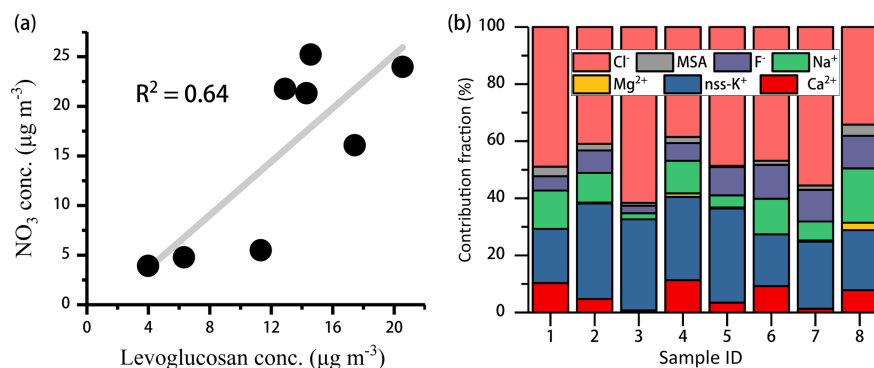


Figure 2. (a) Correlation analysis between the mass concentrations of levoglucosan and aerosol nitrate during the Sanjiang sampling campaign; (b) variation of fractions of various inorganic species (MSA^- stands for methyl sulphonate) during day–night samplings at Sanjiang between 8 and 18 October 2013 (sample ID 1 to 8). The higher relative abundances of nss-K^+ and Cl^- are indicative of a biomass-burning-dominated source. For sample ID information and exact sampling dates, refer to Table S3.

cosan in Sanjiang was indeed pristine and represented a reliable source indicator that is unbiased by altering processes in the atmosphere. Moreover, in our previous work (Cao et al., 2017), we observed that there was a much greater enhancement of atmospheric NO_3^- compared to SO_4^{2-} (a typical coal-related pollutant). This additionally points to biomass burning, and not coal-combustion, as the dominant $p\text{NO}_3^-$ source in the study area, making SJ an ideal “quasi-single-source” environment for calibrating the N isotope effect during $p\text{NO}_3^-$ formation.

Our $\delta^{18}\text{O}$ – $p\text{NO}_3^-$ values are well within the broad range of values in previous reports (Zong et al., 2017; Geng et al., 2017; Walters and Michalski, 2016). However, as depicted in Fig. 3, the $\delta^{15}\text{N}$ values of biomass-burning-emitted NO_3^- fall within the range of $\delta^{15}\text{N}$ – NO_x values typically reported for emissions from coal combustion, whereas they are significantly higher than the well-established values for $\delta^{15}\text{N}$ – NO_x emitted from the burning of various types of biomass (mean: $1.04 \pm 4.13\text{‰}$; range: -7 to $+12\text{‰}$) (Fibiger and Hastings, 2016). Turekian et al. (1998) conducted laboratory tests involving the burning of eucalyptus and African grasses, and determined that the $\delta^{15}\text{N}$ of $p\text{NO}_3^-$ (around 23‰) was 6.6‰ higher than the $\delta^{15}\text{N}$ of the burned biomass. This implies significant N isotope partitioning during biomass burning. In the case of complete biomass combustion, by mass balance, the first gaseous products (i.e., NO_x) have the same $\delta^{15}\text{N}$ as the biomass. Hence any discrepancy between the $p\text{NO}_3^-$ and the $\delta^{15}\text{N}$ of the biomass can be attributed to the N isotope fractionation associated with the partial conversion of gaseous NO_x to aerosol NO_3^- . Based on the computational quantum chemistry (CQC) module calculations, the N isotope fractionation ϵ_{N} (mean $_{\text{min}}^{\text{max}} \pm 1\sigma$) determined from the Sanjiang data was $10.99_{10.30}^{12.54} \pm 0.74\text{‰}$. After correcting the primary $\delta^{15}\text{N}$ – $p\text{NO}_3^-$ values under the consideration of ϵ_{N} , the resulting mean $\delta^{15}\text{N}$ of $1.17_{-1.89}^{2.98} \pm 1.95\text{‰}$ is very close to the N isotopic signature expected for biomass-burning-emitted NO_x ($1.04 \pm 4.13\text{‰}$) (Fig. 3) (Fibiger and Hastings, 2016).

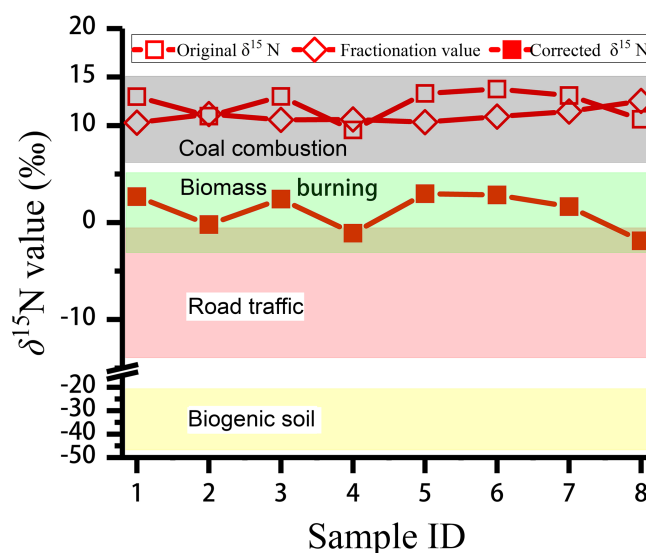


Figure 3. Original $\delta^{15}\text{N}$ values ($\delta^{15}\text{N}_{\text{ini}}$) for $p\text{NO}_3^-$, calculated values for the N isotope fractionation (ϵ_{N}) associated with the conversion of gaseous NO_x to $p\text{NO}_3^-$ and corrected $\delta^{15}\text{N}$ values ($\delta^{15}\text{N}_{\text{corr}}$; $^{15}\text{N}_{\text{ini}}$ minus ϵ_{N}) of $p\text{NO}_3^-$ for each sample collected during the Sanjiang sampling campaign. The colored bands represent the variation range of $\delta^{15}\text{N}$ values for different NO_x sources based on reports from the literature (Table S2). See Table S3 for the information regarding sample ID.

The much higher $\delta^{15}\text{N}$ – $p\text{NO}_3^-$ values in our study compared to reported $\delta^{15}\text{N}$ – NO_x values for biomass burning can easily be reconciled when including N isotope fractionation during the conversion of NO_x to NO_3^- . Put another way, given that Sanjiang is an environment where we can essentially exclude NO_x sources other than biomass burning at the time of sampling, the data nicely validate our CQC-module-based approach to estimating ϵ_{N} .

4.2 Source apportionment of NO_x in an urban setting using a Bayesian isotopic mixing model

Due to its high population density and intensive industrial production, the Nanjing atmosphere was expected to have high NO_x concentrations derived from road traffic and coal combustion (Zhao et al., 2015). However, the raw $\delta^{15}\text{N}-p\text{NO}_3^-$ values ($10.93 \pm 3.32\text{‰}$) fell well within the variation range of coal-emitted $\delta^{15}\text{N}-\text{NO}_x$ (Fig. 3). It is tempting to conclude that coal combustion is the main, or even sole, $p\text{NO}_3^-$ source (given the equivalent $\delta^{15}\text{N}$ values), yet this is very unlikely. The data rather confirm that significant isotope fractionation occurred during the conversion of NO_x to NO_3^- and that, without consideration of the N isotope effect, traffic-related NO_x emissions will be markedly underestimated.

In the atmosphere, the oxygen atoms of NO_x rapidly exchanged with O_3 in the “ $\text{NO}-\text{NO}_2$ ” cycle (see Reactions R1–R3) (Hastings et al., 2003), and the $\delta^{18}\text{O}-p\text{NO}_3^-$ values are determined by its production pathways (Reactions R4–R7), rather than the sources of NO_x (Hastings et al., 2003). Thus, $\delta^{18}\text{O}-p\text{NO}_3^-$ can be used to gain information on the pathway of conversion of NO_x to nitrate in the atmosphere (Fang et al., 2011). In the computational quantum chemistry module used here to calculate isotope fractionation, we assumed that two-thirds of the oxygen atoms in NO_3^- derive from O_3 and one-third from $\bullet\text{OH}$ in the $\bullet\text{OH}$ generation pathway (Reaction R4) (Hastings et al., 2003); correspondingly, five-sixths of the oxygen atoms then derived from O_3 and one-sixth from $\bullet\text{OH}$ in the “ $\text{O}_3-\text{H}_2\text{O}$ ” pathway (Reactions R5–R7). The assumed range for $\delta^{18}\text{O}-\text{O}_3$ and $\delta^{18}\text{O}-\text{H}_2\text{O}$ values were $90\text{‰}-122\text{‰}$ and $-25\text{‰}-0\text{‰}$, respectively (Zong et al., 2017). The partitioning between the two possible pathways was then assessed through Monte Carlo simulation (Zong et al., 2017). The estimated range was rather broad, given the wide range of $\delta^{18}\text{O}-\text{O}_3$ and $\delta^{18}\text{O}-\text{H}_2\text{O}$ values used. Nevertheless, the theoretical calculation of the average contribution ratio (γ) for nitrate formation in Nanjing via the reaction of NO_2 and $\bullet\text{OH}$ is consistent with the results from simulations using the Weather Research and Forecasting model coupled with Chemistry (WRF-Chem) (Fig. 4; see Sect. S3 for details). A clear diurnal cycle of the mass concentration of nitrate formed through $\bullet\text{OH}$ oxidation of NO_2 can be observed (Fig. S3), with much higher concentrations between 12:00 and 18:00. This indicates the importance of photochemically produced $\bullet\text{OH}$ during daytime. Yet, throughout our sampling period in Nanjing, the average $p\text{NO}_3^-$ formation by the heterogeneous hydrolysis of N_2O_5 ($12.6 \mu\text{g mm}^{-3}$) exceeded $p\text{NO}_3^-$ formation by the reaction of NO_2 and $\bullet\text{OH}$ ($4.8 \mu\text{g mm}^{-3}$), even during daytime, consistent with recent observations during peak pollution periods in Beijing (Wang et al., 2017). Given the production rates of N_2O_5 in the atmosphere are governed by ambient O_3 concentrations, reducing atmospheric O_3 levels appears to be one of the most

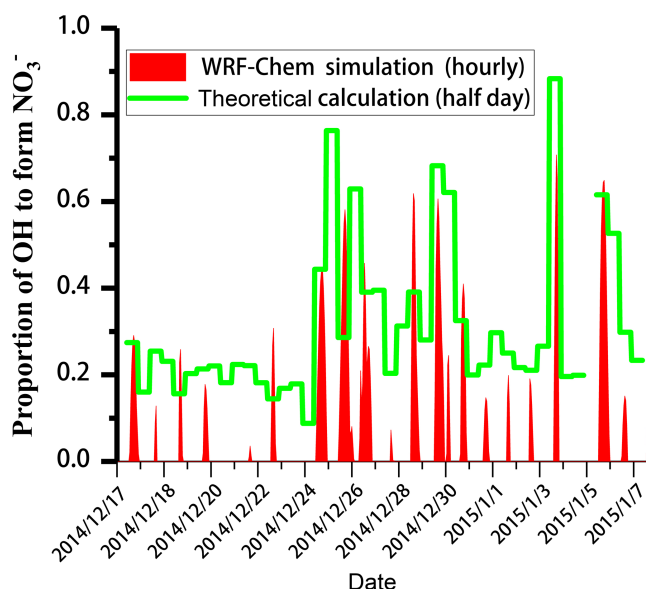


Figure 4. Comparison between the theoretical calculation and WRF-Chem simulation of the average contribution ratio (γ) for nitrate formation in Nanjing via the reaction of NO_2 and photochemically produced $\bullet\text{OH}$.

important measures to take for mitigating $p\text{NO}_3^-$ pollution in China’s urban atmospheres.

In Nanjing, dependent on the time-dependent, dominant $p\text{NO}_3^-$ formation pathway, the average N isotope fractionation value calculated using the computational quantum chemistry module varied between 10.77‰ and 19.34‰ (15.33‰ on average). Using the Bayesian model MixSIR, the contribution of each source can be estimated, based on the mixed-source isotope data under the consideration of prior information at the site (see Sect. S1 for detailed information regarding model frame and computing method). As described above, theoretically, there are four major sources potentially contributing to ambient NO_x : road traffic, coal combustion, biomass burning and biogenic soil. As a start, we tentatively integrated all four sources into MixSIR (data not shown). The relative contribution of biomass burning to the ambient NO_x (median value) ranged from 28 % to 70 % (average 42 %), representing the most important source. The primary reason for such apparently high contribution by biomass burning is that the corrected $\delta^{15}\text{N}-p\text{NO}_3^-$ values of $-4.29_{-10.32}^{0.42} \pm 3.66\text{‰}$ are relatively close to the N isotopic signature of biomass-burning-emitted NO_x ($1.04 \pm 4.13\text{‰}$) compared to the other possible sources. Based on $\delta^{15}\text{N}$ alone, the isotope approach can be ambiguous if there are more than two sources. The N isotope signature of NO_x from biomass burning falls right in between the spectrum of plausible values, with highest $\delta^{15}\text{N}$ for emissions from coal combustion on the one end and much lower values for automotive and soil emissions on the other, and will be similar to a mixed signature from coal combustion and NO_x emissions from traffic.

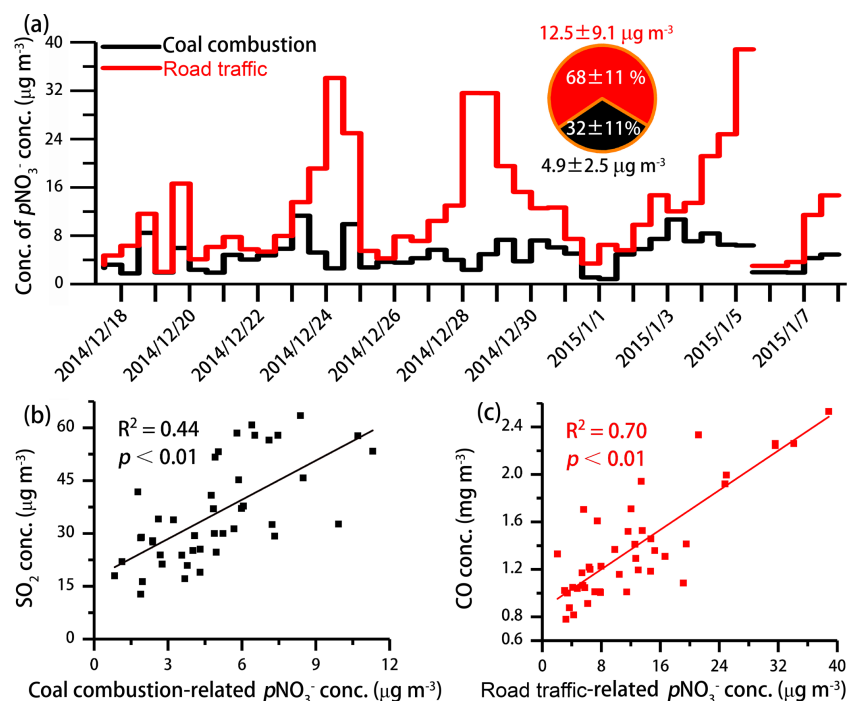


Figure 5. (a) Time-series variation of coal combustion and road traffic contribution to the mass concentrations of ambient $p\text{NO}_3^-$ in Nanjing, as estimated through MixSIR; (b) correlation analysis between the mass concentrations of coal-combustion-related $p\text{NO}_3^-$ and SO_2 ; (c) correlation analysis between the mass concentrations of road-traffic-related $p\text{NO}_3^-$ and CO.

We can make several evidence-based presumptions to better constrain the emission sources in the mixing model analysis: (1) when sampling at a typical urban site in a major industrial city in China, we can assume that the sources of road traffic and coal combustion are dominant, while the contribution of biogenic soil to ambient NO_x should have minimal impact or can be largely neglected (Zhao et al., 2015); (2) there is no crop harvest activity in eastern China during the winter season. Furthermore, deforestation and combustion of fuelwood have been discontinued in China's major cities (Chang et al., 2016a). Therefore, the contribution of biomass-burning-emitted NO_x during the sampling period should also be minor. Indeed, Fig. S4 shows that the mass concentration of biomass-burning-related $p\text{NO}_3^-$ is not correlated with the fraction of levoglucosan that contributes to OC, confirming a weak impact of biomass burning on the variation of $p\text{NO}_3^-$ concentration during our study period.

In a second, alternative and more realistic scenario, we excluded biomass burning and soil as a potential source of NO_x in MixSIR (see above). As illustrated in Fig. 5a, assuming that NO_x emissions in urban Nanjing during our study period originated solely from road traffic and coal combustion, their relative contribution to the mass concentration of $p\text{NO}_3^-$ is $12.5 \pm 9.1 \mu\text{g m}^{-3}$ (or $68 \pm 11\%$) and $4.9 \pm 2.5 \mu\text{g m}^{-3}$ (or $32 \pm 11\%$), respectively. These numbers agree well with a city-scale NO_x emission inventory established for Nanjing recently (Zhao et al., 2015). Nevertheless, on a nation-wide

level, relatively large uncertainties with regards to the overall fossil fuel consumption and fuel types propagate into large uncertainties of NO_x concentration estimates and predictions of longer-term emission trends (Li et al., 2017). Current emission-inventory estimates (Jaegle et al., 2005; Zhang et al., 2012; Liu et al., 2015; Zhao et al., 2013) suggest that in 2010 NO_x emissions from coal-fired power plants in China were about 30% higher than those from transportation. However, our isotope-based source apportionment of NO_x clearly shows that in 2014 the contribution from road traffic to NO_x emissions, at least in Nanjing (a city that can be considered representative for most densely populated areas in China), is twice that of coal combustion. In fact, due to changing economic activities, emission sources of air pollutants in China are changing rapidly. For example, over the past several years, China has implemented an extended portfolio of plans to phase out its old-fashioned and small power plants, and to raise the standards for reducing industrial pollutant emissions (Chang, 2012). On the other hand, China continuously experienced double-digit annual growth in terms of auto sales during the 2000s, and in 2009 it became the world's largest automobile market (X. Liu et al., 2013; Chang et al., 2017, 2016b). Recent satellite-based studies have successfully analyzed the NO_x vertical column concentration ratios for megacities in eastern China and highlighted the importance of transportation-related NO_x emissions (Reuter et al., 2014; Gu et al., 2014; Duncan et al., 2016; Jin et

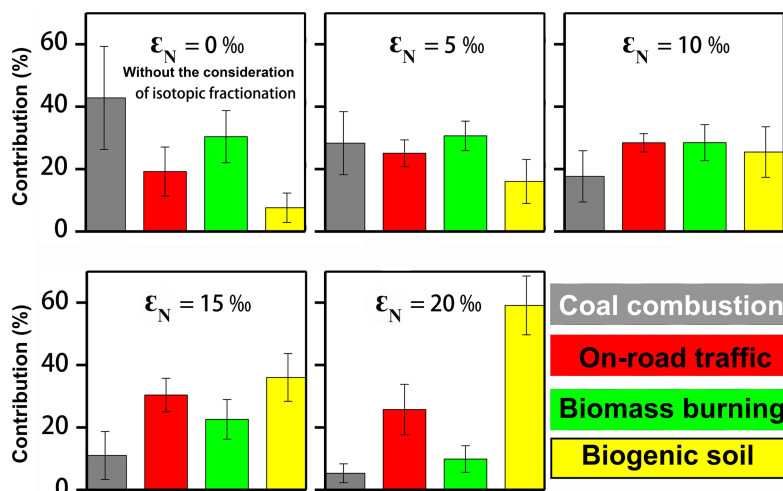


Figure 6. Estimates of the relative importance of single NO_x sources (mean $\pm 1\sigma$) throughout China based on the original $\delta^{15}\text{N}\text{-NO}_3^-$ values extracted from the literature ($\epsilon_N = 0\text{‰}$) and under consideration of significant N isotope fractionation during NO_x transformation ($\epsilon_N = 5\text{‰}$, 10‰ , 15‰ or 20‰).

al., 2017). Moreover, long-term measurements of the ratio of NO_3^- to non-sea-salt SO_4^{2-} in precipitation and aerosol jointly revealed a continuously increasing trend in eastern China throughout the latest decade, suggesting decreasing emissions from coal combustion (X. Liu et al., 2013; Itahashi et al., 2018). Both coal-combustion- and road-traffic-related $p\text{NO}_3^-$ concentrations are highly correlated with their corresponding tracers (i.e., SO_2 and CO , respectively), confirming the validity of our MixSIR modeling results. With justified confidence in our Bayesian isotopic model results, we conclude that previous estimates of NO_x emissions from automotive/transportation sources in China based on bottom-up emission inventories may be too low.

4.3 Previous $\delta^{15}\text{N}\text{-NO}_3^-$ -based estimates on NO_x sources

Stable nitrogen isotope ratios of nitrate have been used to identify nitrogen sources in various environments in China, often without large differences in $\delta^{15}\text{N}$ between rainwater and aerosol NO_3^- (Kojima et al., 2011). In previous work, no consideration was given to potential N isotope fractionation during atmospheric $p\text{NO}_3^-$ formation. Here, we reevaluated 700 data points of $\delta^{15}\text{N}\text{-NO}_3^-$ in aerosol ($-0.77 \pm 4.52\text{‰}$; $n = 308$) and rainwater ($3.79 \pm 6.14\text{‰}$; $n = 392$) from 13 sites that are located in the area of mainland China and the Yellow, East China and South China seas (Fig. 1), extracted from the literature (see Table S4 for details). To verify the potentially biasing effects of neglecting N isotope fractionation (i.e., testing the sensitivity of ambient NO_x source contribution estimates to the effect of N isotope fractionation), the Bayesian isotopic mixing model was applied (a) to the original NO_3^- isotope data set and (b) to the corrected nitrate isotope data set, accounting for the N isotope fractionation dur-

ing NO_x transformation. All 13 sampling sites are located in non-urban areas; therefore, apart from coal combustion and on-road traffic, the contributions of biomass burning and biogenic soil to nitrate need to be taken into account.

Although most of the sites are located in rural and coastal environments, when the original data set is used without the consideration of N isotope fractionation in the Bayesian isotopic mixing model, fossil-fuel-related NO_x emissions (coal combustion and on-road traffic) appear to be the largest contributor at all the sites (data are not shown). This is particularly true for coal combustion: everywhere except for the sites of Dongshan islands and Mt. Lumin, NO_x emissions seem to be dominated by coal combustion. Very high contribution from coal combustion (on the order of 40%–60%) particularly in northern China may be plausible and can be attributed to a much larger consumption of coal. Yet, rather unlikely, the highest estimated contribution of coal combustion (83%) was calculated for Beihuang Island (a full-year sampling on a coastal island that is 65 km north of Shandong Peninsula and 185 km east of the Beijing–Tianjin–Hebei region) and not for mainland China. While Beihuang may be an extreme example, we argue that, collectively, the contribution of coal combustion to ambient NO_x in China as calculated on the basis of isotopic analyses in previous studies without the consideration of N isotope fractionation represents overestimates.

As a first step towards a more realistic assessment of the actual partitioning of NO_x sources in China in general (and coal-combustion-emitted NO_x in particular), it is imperative to determine the location-specific values for ϵ_N . Unfortunately, without $\delta^{18}\text{O}\text{-NO}_3^-$ data on hand, or data on meteorological parameters that correspond to the 700 $\delta^{15}\text{N}\text{-NO}_3^-$ values used in our meta-analysis, it is not possible to esti-

mate the ϵ_N values through the abovementioned CQC module. As a viable alternative, we adopted the approximate values for ϵ_N as estimated in Sanjiang (10.99‰) and Nanjing (15.33 ± 4.90‰). As indicated in Fig. 6, the estimates of the source partitioning are sensitive to the choice of ϵ_N . Whereas, with increasing ϵ_N , estimates on the relative contribution of on-road traffic and biomass burning remained relatively stable, estimates for coal combustion and biogenic soil changed significantly, in opposite directions. More precisely, depending on ϵ_N , the average estimate of the fractional contribution of coal combustion decreased drastically from 43 % ($\epsilon_N = 0\%$) to 5 % ($\epsilon_N = 20\%$) (Fig. 6), while the contribution from biogenic soil to NO_x emissions increased in a complementary way. Given the lack of better constraints on ϵ_N for the 13 sampling sites, it cannot be our goal here to provide a robust revised estimate on the partitioning of NO_x sources throughout China and its neighboring areas. But we have very good reasons to assume that disregard of N isotope fractionation during $p\text{NO}_3^-$ formation in previous isotope-based source apportionment studies has likely led to overestimates of the relative contribution of coal combustion to total NO_x emissions in China. For what we would consider the most conservative estimate, i.e., lowest calculated value for the N isotope fractionation during the transformation of NO_x to $p\text{NO}_3^-$ ($\epsilon_N = 5\%$), the approximate contribution from coal combustion to the NO_x pool would be 28 %, more than 30 % less than N-isotope-mixing-model-based estimates would yield without consideration of the N isotope fractionation (i.e., $\epsilon_N = 0\%$) (Fig. 6).

5 Conclusion and outlook

Consistent with theoretical predictions, $\delta^{15}\text{N}$ - $p\text{NO}_3^-$ data from a field experiment where atmospheric $p\text{NO}_3^-$ formation could be attributed reliably to NO_x solely from biomass burning revealed that the conversion of NO_x to $p\text{NO}_3^-$ is associated with a significant net N isotope effect (ϵ_N). It is imperative that future studies, making use of isotope mixing models to gain conclusive constraints on the source partitioning of atmospheric NO_x , consider this N isotope fractionation. The latter will change with time and space, depending on the distribution of ozone and OH radicals in the atmosphere and the predominant NO_x chemistry. The O isotope signatures of $p\text{NO}_3^-$ is mostly chemistry (and not source) driven (modulated by O isotope exchange reactions in the atmosphere), and thus O isotope measurements do not allow addressing the ambiguities with regards to the NO_x source that may remain when just looking at $\delta^{15}\text{N}$ values alone. However, $\delta^{18}\text{O}$ in $p\text{NO}_3^-$ will help in assessing the relative importance of the dominant $p\text{NO}_3^-$ formation pathway. Simultaneous $\delta^{15}\text{N}$ and $\delta^{18}\text{O}$ measurements of atmospheric nitrate thus allow reliable information on ϵ_N and in turn on the relative importance of single NO_x sources. For example, for Nanjing, which can be considered representative

for other large cities in China, dual-isotopic and chemical-tracer evidence suggest that on-road traffic and coal-fired power plants, rather than biomass burning, are the predominant sources during high-haze pollution periods. Given that the increasing frequency of nitrate-driven haze episodes in China, our findings are critically important in terms of guiding the use of stable nitrate isotope measurements to evaluate the relative importance of single NO_x sources on regional scales and for adapting suitable mitigation measures. Future assessments of NO_x emissions in China (and elsewhere) should involve simultaneous $\delta^{15}\text{N}$ and $\delta^{18}\text{O}$ measurements of atmospheric nitrate and NO_x at high spatiotemporal resolution, allowing us to more quantitatively reevaluate former N-isotope-based NO_x source partitioning estimates.

Data availability. Data are available from the corresponding author on request. We prefer not to publish the software for calculating the nitrogen isotope fractionation factor and estimating nitrate source attribution at the present stage in order to avoid compromising the future of ongoing software registration. Readers can download the software through the website <http://www.atmosgeochem.com/> (last access: 1 August 2018) after the completion of software registration.

The Supplement related to this article is available online at <https://doi.org/10.5194/acp-18-11647-2018-supplement>.

Author contributions. YZ conceived the study. YZ, ML and YC designed the experimental strategy. YC, CT, XM, FC, SZ, ML and TK performed the geochemical and isotope measurements, analyzed the experimental data and constructed the model. YC and YZ proposed the hypotheses. XL and WZ assisted with the laboratory work. YC wrote the manuscript with ML and YZ; all other co-authors contributed to the data interpretation and writing.

Competing interests. The authors declare that they have no conflict of interest.

Special issue statement. This article is part of the special issue “Multiphase chemistry of secondary aerosol formation under severe haze”. It is not associated with a conference.

Acknowledgements. This study was supported by the National Key Research and Development Program of China (2017YFC0210101), the National Natural Science Foundation of China (grant nos. 91644103, 41705100 and 41575129), the Provincial Natural Science Foundation of Jiangsu (BK20170946), the University Science Research Project of Jiangsu Province (17KJB170011), the International Joint Laboratory on Climate and Environment Change (ILCEC) and the Collaborative Innovation Center on Forecast and Evaluation of Meteorological Disasters (CIC-FEMD) through

NUIST and through University of Basel research funds.

Edited by: Daniel Knopf

Reviewed by: two anonymous referees

References

- Alexander, B., Hastings, M. G., Allman, D. J., Dachs, J., Thornton, J. A., and Kunasek, S. A.: Quantifying atmospheric nitrate formation pathways based on a global model of the oxygen isotopic composition ($\Delta^{17}\text{O}$) of atmospheric nitrate, *Atmos. Chem. Phys.*, 9, 5043–5056, <https://doi.org/10.5194/acp-9-5043-2009>, 2009.
- Altieri, K. E., Hastings, M. G., Gobel, A. R., Peters, A. J., and Sigman, D. M.: Isotopic composition of rainwater nitrate at Bermuda: the influence of air mass source and chemistry in the marine boundary layer, *J. Geophys. Res.*, 118, 11304–311316, <https://doi.org/10.1002/jgrd.50829>, 2013.
- Anenberg, S. C., Miller, J., Minjares, R., Du, L., Henze, D. K., Lacey, F., Malley, C. S., Emberson, L., Franco, V., Klimont, Z., and Heyes, C.: Impacts and mitigation of excess diesel-related NO_x emissions in 11 major vehicle markets, *Nature*, 545, 467–471, <https://doi.org/10.1038/nature22086>, 2017.
- Böhlke, J. K., Mroczkowski, S. J., and Coplen, T. B.: Oxygen isotopes in nitrate: new reference materials for ¹⁸O:¹⁷O:¹⁶O measurements and observations on nitrate-water equilibration, *Rapid Commun. Mass Sp.*, 17, 1835–1846, <https://doi.org/10.1002/rcm.1123>, 2003.
- Cao, F., Zhang, S. C., Kawamura, K., and Zhang, Y. L.: Inorganic markers, carbonaceous components and stable carbon isotope from biomass burning aerosols in Northeast China, *Sci. Total Environ.*, 572, 1244–1251, <https://doi.org/10.1016/j.scitotenv.2015.09.099>, 2016.
- Cao, F., Zhang, S. C., Kawamura, K., Liu, X., Yang, C., Xu, Z., Fan, M., Zhang, W., Bao, M., Chang, Y., Song, W., Liu, S., Lee, X., Li, J., Zhang, G., and Zhang, Y. L.: Chemical characteristics of dicarboxylic acids and related organic compounds in PM_{2.5} during biomass-burning and non-biomass-burning seasons at a rural site of Northeast China, *Environ. Pollut.*, 231, 654–662, <https://doi.org/10.1016/j.envpol.2017.08.045>, 2017.
- Casciotti, K. L., Sigman, D. M., Hastings, M. G., Böhlke, J. K., and Hilkert, A.: Measurement of the oxygen isotopic composition of nitrate in seawater and freshwater using the denitrifier method, *Anal. Chem.*, 74, 4905–4912, <https://doi.org/10.1021/ac020113w>, 2002.
- Chang, Y., Liu, X., Deng, C., Dore, A. J., and Zhuang, G.: Source apportionment of atmospheric ammonia before, during, and after the 2014 APEC summit in Beijing using stable nitrogen isotope signatures, *Atmos. Chem. Phys.*, 16, 11635–11647, <https://doi.org/10.5194/acp-16-11635-2016>, 2016a.
- Chang, Y., Zou, Z., Deng, C., Huang, K., Collett, J. L., Lin, J., and Zhuang, G.: The importance of vehicle emissions as a source of atmospheric ammonia in the megacity of Shanghai, *Atmos. Chem. Phys.*, 16, 3577–3594, <https://doi.org/10.5194/acp-16-3577-2016>, 2016b.
- Chang, Y., Deng, C., Cao, F., Cao, C., Zou, Z., Liu, S., Lee, X., Li, J., Zhang, G., and Zhang, Y.: Assessment of carbonaceous aerosols in Shanghai, China – Part 1: long-term evolution, seasonal variations, and meteorological effects, *Atmos. Chem. Phys.*, 17, 9945–9964, <https://doi.org/10.5194/acp-17-9945-2017>, 2017.
- Chang, Y. H.: China needs a tighter PM_{2.5} limit and a change in priorities, *Environ. Sci. Technol.*, 46, 7069–7070, <https://doi.org/10.1021/es3022705>, 2012.
- Duncan, B. N., Lamsal, L. N., Thompson, A. M., Yoshida, Y., Lu, Z., Streets, D. G., Hurwitz, M. M., and Pickering, K. E.: A space-based, high-resolution view of notable changes in urban NO_x pollution around the world (2005–2014), *J. Geophys. Res.*, 121, 976–996, <https://doi.org/10.1002/2015JD024121>, 2016.
- Elliott, E., Kendall, C., Wankel, S. D., Burns, D., Boyer, E., Harlin, K., Bain, D., and Butler, T.: Nitrogen isotopes as indicators of NO_x source contributions to atmospheric nitrate deposition across the midwestern and northeastern United States, *Environ. Sci. Technol.*, 41, 7661–7667, <https://doi.org/10.1021/es070898t>, 2007.
- Elliott, E. M., Kendall, C., Boyer, E. W., Burns, D. A., Lear, G. G., Golden, H. E., Harlin, K., Bytnerowicz, A., Butler, T. J., and Glatz, R.: Dual nitrate isotopes in dry deposition: Utility for partitioning NO_x source contributions to landscape nitrogen deposition, *J. Geophys. Res.*, 114, G04020, <https://doi.org/10.1029/2008jg000889>, 2009.
- Fang, Y. T., Koba, K., Wang, X. M., Wen, D. Z., Li, J., Takebayashi, Y., Liu, X. Y., and Yoh, M.: Anthropogenic imprints on nitrogen and oxygen isotopic composition of precipitation nitrate in a nitrogen-polluted city in southern China, *Atmos. Chem. Phys.*, 11, 1313–1325, <https://doi.org/10.5194/acp-11-1313-2011>, 2011.
- Felix, J. D. and Elliott, E. M.: Isotopic composition of passively collected nitrogen dioxide emissions: Vehicle, soil and livestock source signatures, *Atmos. Environ.*, 92, 359–366, <https://doi.org/10.1016/j.atmosenv.2014.04.005>, 2014.
- Felix, J. D., Elliott, E. M., and Shaw, S. L.: Nitrogen isotopic composition of coal-fired power plant NO_x: Influence of emission controls and implications for global emission inventories, *Environ. Sci. Technol.*, 46, 3528–3535, <https://doi.org/10.1021/es203355v>, 2012.
- Felix, J. D., Elliott, E. M., Gish, T. J., McConnell, L. L., and Shaw, S. L.: Characterizing the isotopic composition of atmospheric ammonia emission sources using passive samplers and a combined oxidation-bacterial denitrifier approach, *Rapid Commun. Mass Sp.*, 27, 2239–2246, <https://doi.org/10.1002/rcm.6679>, 2013.
- Fibiger, D. L. and Hastings, M. G.: First measurements of the nitrogen isotopic composition of NO_x from biomass burning, *Environ. Sci. Technol.*, 50, 11569–11574, <https://doi.org/10.1021/acs.est.6b03510>, 2016.
- Freyer, H. D.: Seasonal trends of NH₄⁺ and NO₃⁻ nitrogen isotope composition in rain collected at Jülich, Germany, *Tellus*, 30, 83–92, 1978.
- Freyer, H. D.: Seasonal variation of ¹⁵N/¹⁴N ratios in atmospheric nitrate species, *Tellus*, 43, 30–44, <https://doi.org/10.3402/tellusb.v43i1.15244>, 2017.
- Freyer, H. D., Kley, D., Volz-Thomas, A., and Kobel, K.: On the interaction of isotopic exchange processes with photochemical reactions in atmospheric oxides of nitrogen, *J. Geophys. Res.*, 98, 14791–14796, <https://doi.org/10.1029/93JD00874>, 1993.

- Fu, X., Wang, S., Zhao, B., Xing, J., Cheng, Z., Liu, H., and Hao, J.: Emission inventory of primary pollutants and chemical speciation in 2010 for the Yangtze River Delta region, China, *Atmos. Environ.*, 70, 39–50, <https://doi.org/10.1016/j.atmosenv.2012.12.034>, 2013.
- Galloway, J. N., Aber, J. D., Erisman, J. W., Seitzinger, S. P., Howarth, R. W., Cowling, E. B., and Cosby, B. J.: The nitrogen cascade, *Bioscience*, 53, 341–356, [https://doi.org/10.1641/0006-3568\(2003\)053\[0341:Tnc\]2.0.Co;2](https://doi.org/10.1641/0006-3568(2003)053[0341:Tnc]2.0.Co;2), 2003.
- Geng, L., Murray, L. T., Mickley, L. J., Lin, P., Fu, Q., Schauer, A. J., and Alexander, B.: Isotopic evidence of multiple controls on atmospheric oxidants over climate transitions, *Nature*, 546, 133–136, <https://doi.org/10.1038/nature22340>, 2017.
- Gobel, A. R., Altieri, K. E., Peters, A. J., Hastings, M. G., and Sigman, D. M.: Insights into anthropogenic nitrogen deposition to the North Atlantic investigated using the isotopic composition of aerosol and rainwater nitrate, *Geophys. Res. Lett.*, 40, 5977–5982, <https://doi.org/10.1002/2013GL058167>, 2013.
- Gu, D., Wang, Y., Smeltzer, C., and Boersma, K. F.: Anthropogenic emissions of NO_x over China: Reconciling the difference of inverse modeling results using GOME-2 and OMI measurements, *J. Geophys. Res.*, 119, 7732–7740, <https://doi.org/10.1002/2014JD021644>, 2014.
- Hastings, M. G., Sigman, D. M., and Lipschultz, F.: Isotopic evidence for source changes of nitrate in rain at Bermuda, *J. Geophys. Res.*, 108, 4790, <https://doi.org/10.1029/2003JD003789>, 2003.
- Heaton, T. H. E.: ¹⁵N/¹⁴N ratios of NO_x from vehicle engines and coal-fired power stations, *Tellus*, 42, 304–307, <https://doi.org/10.1034/j.1600-0889.1990.00007.x-i1>, 1990.
- Hennigan, C. J., Sullivan, A. P., Collett, J. L., and Robinson, A. L.: Levoglucosan stability in biomass burning particles exposed to hydroxyl radicals, *Geophys. Res. Lett.*, 37, L09806, <https://doi.org/10.1029/2010GL043088>, 2010.
- Hoering, T.: The isotopic composition of the ammonia and the nitrate ion in rain, *Geochim. Cosmochim. Ac.*, 12, 97–102, [https://doi.org/10.1016/0016-7037\(57\)90021-2](https://doi.org/10.1016/0016-7037(57)90021-2), 1957.
- Itahashi, S., Yumimoto, K., Uno, I., Hayami, H., Fujita, S.-I., Pan, Y., and Wang, Y.: A 15-year record (2001–2015) of the ratio of nitrate to non-sea-salt sulfate in precipitation over East Asia, *Atmos. Chem. Phys.*, 18, 2835–2852, <https://doi.org/10.5194/acp-18-2835-2018>, 2018.
- Jaegle, L., Steinberger, L., Martin, R. V., and Chance, K.: Global partitioning of NO_x sources using satellite observations: Relative roles of fossil fuel combustion, biomass burning and soil emissions, *Faraday Discuss.*, 130, 407–423, <https://doi.org/10.1039/B502128F>, 2005.
- Jedynska, A., Hoek, G., Wang, M., Eeftens, M., Cyrys, J., Beelen, R., Cirach, M., De Nazelle, A., Nystad, W., Makarem Akhlaghi, H., Meliefste, K., Nieuwenhuijsen, M., de Hoogh, K., Brunekreef, B., and Kooter, I. M.: Spatial variations and development of land use regression models of levoglucosan in four European study areas, *Atmos. Chem. Phys. Discuss.*, 14, 13491–13527, <https://doi.org/10.5194/acpd-14-13491-2014>, 2014.
- Ji, S., Cherry, C. R., Zhou, W., Sawhney, R., Wu, Y., Cai, S., Wang, S., and Marshall, J. D.: Environmental justice aspects of exposure to PM_{2.5} emissions from electric vehicle use in China, *Environ. Sci. Technol.*, 49, 13912–13920, <https://doi.org/10.1021/acs.est.5b04927>, 2015.
- Jin, X., Fiore, A. M., Murray, L. T., Valin, L. C., Lamsal, L. N., Duncan, B., Folkert Boersma, K., De Smedt, I., Abad, G. G., Chance, K., and Tonnesen, G. S.: Evaluating a space-based indicator of surface ozone-NO_x-VOC sensitivity over midlatitude source regions and application to decadal trends, *J. Geophys. Res.*, 122, 439–461, <https://doi.org/10.1002/2017JD026720>, 2017.
- Kaiser, J. C., Riemer, N., and Knopf, D. A.: Detailed heterogeneous oxidation of soot surfaces in a particle-resolved aerosol model, *Atmos. Chem. Phys.*, 11, 4505–4520, <https://doi.org/10.5194/acp-11-4505-2011>, 2011.
- Kendall, C., Elliott, E. M., and Wankel, S. D.: Stable isotopes in ecology and environmental science, chap. 12, 2nd Edn., Blackwell, Oxford, 2007.
- Knopf, D. A., Mak, J., Gross, S., and Bertram, A. K.: Does atmospheric processing of saturated hydrocarbon surfaces by NO₃ lead to volatilization?, *Geophys. Res. Lett.*, 33, L17816, <https://doi.org/10.1029/2006GL026884>, 2006.
- Knopf, D. A., Forrester, S. M., and Slade, J. H.: Heterogeneous oxidation kinetics of organic biomass burning aerosol surrogates by O₃, NO₂, N₂O₅, and NO₃, *Phys. Chem. Chem. Phys.*, 13, 21050–21062, <https://doi.org/10.1039/C1CP22478F>, 2011.
- Kojima, K., Murakami, M., Yoshimizu, C., Tayasu, I., Nagata, T., and Furumai, H.: Evaluation of surface runoff and road dust as sources of nitrogen using nitrate isotopic composition, *Chemosphere*, 84, 1716–1722, <https://doi.org/10.1016/j.chemosphere.2011.04.071>, 2011.
- Lamsal, L. N., Martin, R. V., Padmanabhan, A., van Donkelaar, A., Zhang, Q., Sioris, C. E., Chance, K., Kurosu, T. P., and Newchurch, M. J.: Application of satellite observations for timely updates to global anthropogenic NO_x emission inventories, *Geophys. Res. Lett.*, 38, L05810, <https://doi.org/10.1029/2010GL046476>, 2011.
- Leighton, P.: Photochemistry of Air Pollution, Academic, New York, 1961.
- Levy, H., Moxim, W. J., and Kasibhatla, P. S.: A global three-dimensional time-dependent lightning source of tropospheric NO_x, *J. Geophys. Res.*, 101, 22911–22922, <https://doi.org/10.1029/96JD02341>, 1996.
- Li, D. and Wang, X.: Nitrogen isotopic signature of soil-released nitric oxide (NO) after fertilizer application, *Atmos. Environ.*, 42, 4747–4754, <https://doi.org/10.1016/j.atmosenv.2008.01.042>, 2008.
- Li, M., Zhang, Q., Kurokawa, J.-I., Woo, J.-H., He, K., Lu, Z., Ohara, T., Song, Y., Streets, D. G., Carmichael, G. R., Cheng, Y., Hong, C., Huo, H., Jiang, X., Kang, S., Liu, F., Su, H., and Zheng, B.: MIX: a mosaic Asian anthropogenic emission inventory under the international collaboration framework of the MICS-Asia and HTAP, *Atmos. Chem. Phys.*, 17, 935–963, <https://doi.org/10.5194/acp-17-935-2017>, 2017.
- Ling, T. Y. and Chan, C. K.: Formation and transformation of metastable double salts from the crystallization of mixed ammonium nitrate and ammonium sulfate particles, *Environ. Sci. Technol.*, 41, 8077–8083, <https://doi.org/10.1021/es071419t>, 2007.
- Liu, D., Li, J., Zhang, Y., Xu, Y., Liu, X., Ding, P., Shen, C., Chen, Y., Tian, C., and Zhang, G.: The use of levoglucosan and radiocarbon for source apportionment of PM_{2.5} carbonaceous aerosols at a background site in East China, *Environ. Sci. Technol.*, 47, 10454–10461, <https://doi.org/10.1021/es401250k>, 2013.

- Liu, F., Zhang, Q., Tong, D., Zheng, B., Li, M., Huo, H., and He, K. B.: High-resolution inventory of technologies, activities, and emissions of coal-fired power plants in China from 1990 to 2010, *Atmos. Chem. Phys.*, 15, 13299–13317, <https://doi.org/10.5194/acp-15-13299-2015>, 2015.
- Liu, J., Li, J., Zhang, Y., Liu, D., Ding, P., Shen, C., Shen, K., He, Q., Ding, X., Wang, X., Chen, D., Szidat, S., and Zhang, G.: Source apportionment using radiocarbon and organic tracers for PM_{2.5} carbonaceous aerosols in Guangzhou, South China: contrasting local- and regional-scale haze events, *Environ. Sci. Technol.*, 48, 12002–12011, <https://doi.org/10.1021/es503102w>, 2014.
- Liu, X., Zhang, Y., Han, W., Tang, A., Shen, J., Cui, Z., Vitousek, P., Erisman, J. W., Goulding, K., Christie, P., Fangmeier, A., and Zhang, F.: Enhanced nitrogen deposition over China, *Nature*, 494, 459–463, <https://doi.org/10.1038/nature11917>, 2013.
- Lu, Z., Streets, D. G., de Foy, B., Lamsal, L. N., Duncan, B. N., and Xing, J.: Emissions of nitrogen oxides from US urban areas: estimation from Ozone Monitoring Instrument retrievals for 2005–2014, *Atmos. Chem. Phys.*, 15, 10367–10383, <https://doi.org/10.5194/acp-15-10367-2015>, 2015.
- Michalski, G., Scott, Z., Kabling, M., and Thiemens, M. H.: First measurements and modeling of $\Delta^{17}\text{O}$ in atmospheric nitrate, *Geophys. Res. Lett.*, 30, 1870–1872, <https://doi.org/10.1029/2003gl017015>, 2003.
- Miyazaki, K., Eskes, H., Sudo, K., Boersma, K. F., Bowman, K., and Kanaya, Y.: Decadal changes in global surface NO_x emissions from multi-constituent satellite data assimilation, *Atmos. Chem. Phys.*, 17, 807–837, <https://doi.org/10.5194/acp-17-807-2017>, 2017.
- Morin, S., Savarino, J., Frey, M. M., Yan, N., Bekki, S., Bottenheim, J. W., and Martins, J. M.: Tracing the origin and fate of NO_x in the Arctic atmosphere using stable isotopes in nitrate, *Science*, 322, 730–732, <https://doi.org/10.1126/science.1161910>, 2008.
- Morino, Y., Kondo, Y., Takegawa, N., Miyazaki, Y., Kita, K., Komazaki, Y., Fukuda, M., Miyakawa, T., Moteki, N., and Worsnop, D. R.: Partitioning of HNO₃ and particulate nitrate over Tokyo: Effect of vertical mixing, *J. Geophys. Res.*, 111, D15215, <https://doi.org/10.1029/2005JD006887>, 2006.
- Park, Y. M., Park, K. S., Kim, H., Yu, S. M., Noh, S., Kim, M. S., Kim, J. Y., Ahn, J. Y., Lee, M. D., Seok, K. S., and Kim, Y. H.: Characterizing isotopic compositions of TC-C, NO₃⁻-N, and NH₄⁺-N in PM_{2.5} in South Korea: Impact of China's winter heating, *Environ. Pollut.*, 233, 735–744, <https://doi.org/10.1016/j.envpol.2017.10.072>, 2018.
- Parnell, A. C., Phillips, D. L., Bearhop, S., Semmens, B. X., Ward, E. J., Moore, J. W., Jackson, A. L., Grey, J., Kelly, D. J., and Inger, R.: Bayesian stable isotope mixing models, *Environmetrics*, 24, 387–399, <https://doi.org/10.1002/env.2221>, 2013.
- Phillips, D. L., Inger, R., Bearhop, S., Jackson, A. L., Moore, J. W., Parnell, A. C., Semmens, B. X., and Ward, E. J.: Best practices for use of stable isotope mixing models in food-web studies, *Can. J. Zool.*, 92, 823–835, <https://doi.org/10.1139/cjz-2014-0127>, 2014.
- Price, C., Penner, J., and Prather, M.: NO_x from lightning: 1. Global distribution based on lightning physics, *J. Geophys. Res.*, 102, 5929–5941, <https://doi.org/10.1029/96JD03504>, 1997.
- Reuter, M., Buchwitz, M., Hilboll, A., Richter, A., Schneising, O., Hilker, M., Heymann, J., Bovensmann, H., and Burrows, J. P.: Decreasing emissions of NO_x relative to CO₂ in East Asia inferred from satellite observations, *Nat. Geosci.*, 7, 792–795, <https://doi.org/10.1038/ngeo2257>, 2014.
- Richter, A., Burrows, J. P., Nüß, H., Granier, C., and Niemeier, U.: Increase in tropospheric nitrogen dioxide over China observed from space, *Nature*, 437, 129–132, <https://doi.org/10.1038/nature04092>, 2005.
- Savarino, J., Kaiser, J., Morin, S., Sigman, D. M., and Thiemens, M. H.: Nitrogen and oxygen isotopic constraints on the origin of atmospheric nitrate in coastal Antarctica, *Atmos. Chem. Phys.*, 7, 1925–1945, <https://doi.org/10.5194/acp-7-1925-2007>, 2007.
- Seinfeld, J. H. and Pandis, S. N.: *Atmospheric chemistry and physics: From air pollution to climate change*, John Wiley & Sons, 2012.
- Shiraiwa, M., Pöschl, U., and Knopf, D. A.: Multiphase chemical kinetics of NO₃ radicals reacting with organic aerosol components from biomass burning, *Environ. Sci. Technol.*, 46, 6630–6636, <https://doi.org/10.1021/es300677a>, 2012.
- Sigman, D. M., Casciotti, K. L., Andreani, M., Barford, C., Galanter, M., and Böhlke, J. K.: A bacterial method for the nitrogen isotopic analysis of nitrate in seawater and freshwater, *Anal. Chem.*, 73, 4145–4153, <https://doi.org/10.1021/ac010088e>, 2001.
- Simoneit, B. R. T.: Biomass burning – a review of organic tracers for smoke from incomplete combustion, *Appl. Geochem.*, 17, 129–162, [https://doi.org/10.1016/S0883-2927\(01\)00061-0](https://doi.org/10.1016/S0883-2927(01)00061-0), 2002.
- Simoneit, B. R. T., Schauer, J. J., Nolte, C. G., Oros, D. R., Elias, V. O., Fraser, M. P., Rogge, W. F., and Cass, G. R.: Levoglucosan, a tracer for cellulose in biomass burning and atmospheric particles, *Atmos. Environ.*, 33, 173–182, [https://doi.org/10.1016/S1352-2310\(98\)00145-9](https://doi.org/10.1016/S1352-2310(98)00145-9), 1999.
- Smith, M. L., Bertram, A. K., and Martin, S. T.: Deliquescence, efflorescence, and phase miscibility of mixed particles of ammonium sulfate and isoprene-derived secondary organic material, *Atmos. Chem. Phys.*, 12, 9613–9628, <https://doi.org/10.5194/acp-12-9613-2012>, 2012.
- Solomon, S., Qin, D., Manning, M., Chen, Z., Marquis, M., Averyt, K. B., Tignor, M., and Miller, H. L.: *Climate change 2007: The physical science basis: contribution of Working Group I to the Fourth Assessment Report of the Intergovernmental Panel on Climate Change*, Cambridge University Press, New York, 2007.
- Thiemens, M. H.: Mass-independent isotope effects in planetary atmospheres and the early solar system, *Science*, 283, 341–345, <https://doi.org/10.1126/science.283.5400.341>, 1999.
- Thiemens, M. H. and Heidenreich, J. E.: The mass-independent fractionation of oxygen: a novel isotope effect and its possible cosmochemical implications, *Science*, 219, 1073–1075, <https://doi.org/10.1126/science.219.4588.1073>, 1983.
- Turekian, V. C., Macko, S., Ballentine, D., Swap, R. J., and Garstang, M.: Causes of bulk carbon and nitrogen isotope fractionations in the products of vegetation burns: laboratory studies, *Chem. Geol.*, 152, 181–192, [https://doi.org/10.1016/S0009-2541\(98\)00105-3](https://doi.org/10.1016/S0009-2541(98)00105-3), 1998.
- Walters, W. W. and Michalski, G.: Theoretical calculation of nitrogen isotope equilibrium exchange fractionation factors for various NO_y molecules, *Geochim. Cosmochim. Acta.*, 164, 284–297, <https://doi.org/10.1016/j.gca.2015.05.029>, 2015.
- Walters, W. W. and Michalski, G.: Theoretical calculation of oxygen equilibrium isotope fractionation factors involving various NO_y

- molecules, OH, and H₂O and its implications for isotope variations in atmospheric nitrate, *Geochim. Cosmochim. Ac.*, 191, 89–101, <https://doi.org/10.1016/j.gca.2016.06.039>, 2016.
- Walters, W. W., Goodwin, S. R., and Michalski, G.: Nitrogen stable isotope composition ($\delta^{15}\text{N}$) of vehicle-emitted NO_x, *Environ. Sci. Technol.*, 49, 2278–2285, <https://doi.org/10.1021/es505580v>, 2015.
- Walters, W. W., Simonini, D. S., and Michalski, G.: Nitrogen isotope exchange between NO and NO₂ and its implications for $\delta^{15}\text{N}$ variations in tropospheric NO_x and atmospheric nitrate, *Geophys. Res. Lett.*, 43, 440–448, <https://doi.org/10.1002/2015gl066438>, 2016.
- Wang, H., Lu, K., Chen, X., Zhu, Q., Chen, Q., Guo, S., Jiang, M., Li, X., Shang, D., Tan, Z., Wu, Y., Wu, Z., Zou, Q., Zheng, Y., Zeng, L., Zhu, T., Hu, M., and Zhang, Y.: High N₂O₅ concentrations observed in urban Beijing: Implications of a large nitrate formation pathway, *Environ. Sci. Tech. Lett.*, 4, 416–420, <https://doi.org/10.1021/acs.estlett.7b00341>, 2017.
- Wankel, S. D., Chen, Y., Kendall, C., Post, A. F., and Paytan, A.: Sources of aerosol nitrate to the Gulf of Aqaba: Evidence from $\delta^{15}\text{N}$ and $\delta^{18}\text{O}$ of nitrate and trace metal chemistry, *Mar. Chem.*, 120, 90–99, <https://doi.org/10.1016/j.marchem.2009.01.013>, 2010.
- Wojtal, P. K., Miller, D. J., O’Conner, M., Clark, S. C., and Hastings, M. G.: Automated, high-resolution mobile collection system for the nitrogen isotopic analysis of NO_x, *Jove-J. Vis. Exp.*, 118, e54962, <https://doi.org/10.3791/54962>, 2016.
- Yienger, J. J. and Levy, H.: Empirical model of global soil-biogenic NO_x emissions, *J. Geophys. Res.*, 100, 11447–11464, <https://doi.org/10.1029/95JD00370>, 1995.
- Zhang, Q., Geng, G., Wang, S., Richter, A., and He, K.: Satellite remote sensing of changes in NO_x emissions over China during 1996–2010, *Chinese Sci. Bull.*, 57, 2857–2864, <https://doi.org/10.1007/s11434-012-5015-4>, 2012.
- Zhang, R., Tie, X., and Bond, D. W.: Impacts of anthropogenic and natural NO_x sources over the U.S. on tropospheric chemistry, *P. Natl. Acad. Sci. USA*, 100, 1505–1509, <https://doi.org/10.1073/pnas.252763799>, 2003.
- Zhao, B., Wang, S. X., Liu, H., Xu, J. Y., Fu, K., Klimont, Z., Hao, J. M., He, K. B., Cofala, J., and Amann, M.: NO_x emissions in China: historical trends and future perspectives, *Atmos. Chem. Phys.*, 13, 9869–9897, <https://doi.org/10.5194/acp-13-9869-2013>, 2013.
- Zhao, Y., Qiu, L. P., Xu, R. Y., Xie, F. J., Zhang, Q., Yu, Y. Y., Nielsen, C. P., Qin, H. X., Wang, H. K., Wu, X. C., Li, W. Q., and Zhang, J.: Advantages of a city-scale emission inventory for urban air quality research and policy: the case of Nanjing, a typical industrial city in the Yangtze River Delta, China, *Atmos. Chem. Phys.*, 15, 12623–12644, <https://doi.org/10.5194/acp-15-12623-2015>, 2015.
- Zong, Z., Wang, X., Tian, C., Chen, Y., Fang, Y., Zhang, F., Li, C., Sun, J., Li, J., and Zhang, G.: First assessment of NO_x sources at a regional background site in North China using isotopic analysis linked with modeling, *Environ. Sci. Technol.*, 51, 5923–5931, <https://doi.org/10.1021/acs.est.6b06316>, 2017.